Standard Gibbs energy of metabolic reactions: V. Enolase reaction

Thorsten Greinert,[a] Kristina Vogel,[b] Astrid-Ina Seifert,[a] Riko Siewert,[c] Irina V. Andreeva,[c] Sergey P. Verevkin,[c] Thomas Maskow,[b] Gabriele Sadowski,[a] Christoph Held*[a]

[a] Laboratory of Thermodynamics, Department of Biochemical and Chemical Engineering, Technische Universitaet Dortmund, Emil-Figge-Str. 70, 44227 Dortmund, Germany

[b] UFZ - Helmholtz Centre for Environmental Research, Dept. Environmental Microbiology, Leipzig, Permoserstr. 15, D-04318 Leipzig, Germany

[c] Department of Physical Chemistry, University of Rostock, 18059, Rostock, Germany

* corresponding author: christoph.held@tu-dortmund.de

Symbols

Greek letters

Symbol	Property	Unit
Λ_i	fraction of species i	-
$\varepsilon^{A_iB_i}/k_B$	association-energy parameter	K
γ_i^m	generic activity coefficient of component i on molality base	(kg water)·mol^{-1}
γ_i^x	generic activity coefficient of component i on mole fraction base	-
$\gamma_i^{*,m}$	rational activity coefficient of component i on molality base	-
$\gamma_i^{\infty,m}$	generic activity coefficient of component i at infinite dilution on molality base	(kg water)·mol^{-1}
κ^{AiBi}	association-volume parameter	-
σ_i	segment diameter of component i	Å
ϕ	osmotic coefficient	-
ν_i	stoichiometric coefficient of component i	-

Latin letters

Symbol	Property	Unit
a_i	activity of component i	-
A^{res}	residual Helmholtz energy	J

A^{hc}	hard-chain contribution to Helmholtz energy	J
A^{disp}	dispersion contribution to Helmholtz energy	J
A^{assoc}	association contribution to Helmholtz energy	J
A^{ion}	ionic contribution to Helmholtz energy	J
$\Delta^R \mathrm{g}$	Gibbs energy of chemical reaction	J·mol^{-1}
$\Delta^R g'^0$	standard Gibbs energy of biochemical reaction	J·mol^{-1}
$\Delta^R g'^{0,obs}$	observed standard Gibbs energy of biochemical reaction	J·mol^{-1}
$\Delta^R h'^0$	standard enthalpy of biochemical reaction	J·mol^{-1}
$\Delta^g h^0$	standard gas-phase enthalpy of formation	J·mol^{-1}
$\Delta_l^g h^0$	standard vaporization enthalpy	J·mol^{-1}
$\Delta^l h^0$	standard liquid-phase enthalpy of formation	J·mol^{-1}
k_B	Boltzmann constant (1.38·10^{-23}·m^2·kg·s^{-2}·K^{-1})	J·K^{-1}
k_{ij}	binary interaction parameter of components i and j	-
K_a'	thermodynamic equilibrium constant of biochemical reaction	-
K_{Ai}	dissociation constant	mol·(kg water)$^{-1}$
K_γ'	biochemical activity-coefficient ratio of enolase reaction	(kg water)·mol^{-1}
K_m	chemical apparent equilibrium constant on molality-base of enolase reaction	mol·(kg water)$^{-1}$
K_m'	biochemical apparent equilibrium constant on molality-	mol·(kg water)$^{-1}$

	base of enolase reaction	
K_{Mgi}	magnesium complex dissociation constant	mol·(kg water)$^{-1}$
m_i	molality of component i	mol·(kg water)$^{-1}$
$m_i^{t=0}$	initial molality of component i	mol·(kg water)$^{-1}$
m_i^{seg}	segment number of component i	-
M_i	molar mass of component i	g·mol^{-1}
N_i^{assoc}	number of association sites of component i	-
osm	osmolality	mol·(kg water)$^{-1}$
q	charge of an ion	-
R	ideal gas constant (8.314 J·mol^{-1}·K^{-1})	J·mol^{-1}·K^{-1}
T	temperature	K
u_i/k_B	dispersion-energy parameter of component i	K
x_i	mole fraction of component i	-

Abstract

The glycolytic pathway is one of the most important pathways for living organisms, due to its role in energy production and as supplier of precursors for biosynthesis in living cells. This work focuses on determination of the standard Gibbs energy of reaction $\Delta^R g'^0$ of the enolase reaction, the ninth reaction in the glycolysis pathway. Exact $\Delta^R g'^0$ values are required to predict the thermodynamic feasibility of single metabolic reactions or even of metabolic reaction sequences under cytosolic conditions. So-called "apparent" standard data from literature are only valid at specific conditions. Nevertheless, such data are often used in pathway analyses, which might lead to misinterpretation of the results. In this work, equilibrium measurements were combined with activity coefficients in order to obtain new standard values $\Delta^R g'^0$ for the enolase reaction that are independent of the cytosolic conditions. Reaction equilibria were measured at different initial substrate concentrations and temperatures of 298.15, 305.15 and 310.15 K at pH 7. The activity coefficients were predicted using the equation of state electrolyte Perturbed-Chain Statistical Associating Fluid Theory (ePC-SAFT). The ePC-SAFT parameters were taken from literature or fitted to new experimentally determined osmotic coefficients and densities. At 298.15 K and pH 7, a $\Delta^R g'^0$(298.15 K, pH 7) value of -2.8±0.2 kJ mol^{-1} was obtained. This value differs by up to 5 kJ mol^{-1} from literature data. Reasons are the poorly defined "standard" conditions and partly undefined reaction conditions of literature works. Finally, using temperature-dependent equilibrium constants and the van 't Hoff equation, the standard enthalpy of reaction of $\Delta^R h^0$(298.15 K, pH 7) = 27±10 kJ mol^{-1} was determined, and a similar value was found by quantum-chemistry calculations.

Introduction

The second law of thermodynamics explains whether a (bio-)chemical reaction occurs under the prevailing conditions or not. Reactions and reaction sequences with negative Gibbs energy of reaction $\Delta^R g'$ values are thermodynamically feasible, while others are not. The standard Gibbs energy of reaction $\Delta^R g'^0$ is required to calculate $\Delta^R g'$, which is shown in eq. (1).

$$\Delta^R \mathrm{g}' = \Delta^\mathrm{R} \mathrm{g}'^0 + \mathrm{RT} \ln \left(\prod_i a_i^{\nu_i} \right) \tag{1}$$

Especially for the glycolysis pathway, inconsistent standard data exist in literature. Using those data leads to a misinterpretation of glycolysis. More concrete, positive values of $\Delta^R g'$ under present activities in cells were calculated in contrast to the experience that glycolysis obviously occurs under cytosolic conditions *(1–4)*. Thus, in previous works new standard data $\Delta^R g'^0$ were determined in order to rectify the thermodynamic characterization of glycolysis *(5–9)*. The thermodynamic activity-based procedure to obtain consistent standard data will be applied in this work for the enolase reaction shown in eq. (2), which is the ninth reaction in the ten-step metabolism of glycolysis.

$$\text{2-PG} \rightleftharpoons \text{PEP} + \text{H}_2\text{O} \tag{2}$$

For the enolase, the state of the art value of $\Delta^R g'^0$ which is often used is $\Delta^R g'^0$(298.15 K) = 1.7 kJ mol^{-1} (pH unknown, concentrations unknown) *(1,10)*. Nevertheless, a broad range of values is reported in literature *(11–15)* which includes negative and positive values for $\Delta^R g'^0$ that differ by up to 6 kJ mol^{-1}, which leads to the

question, which values are correct and should be used for pathway calculations? Obviously, the large difference in $\Delta^R g'^0$ leads to completely different conclusions about the thermodynamic feasibility of metabolic reactions using eq. (1). One possible reason for this high discrepancy is that authors measured at different conditions. Thus, a precise description of the conditions (T, pH, buffers, ionic strength, substrate concentration) at which the values were measured is required. Unfortunately, this information is often not provided by authors, which makes an evaluation of given literature data even harder. So Wold and Ballou *(15)* determined $\Delta^R g'^0$ = -3.61 kJ mol^{-1} at 298.15 K, pH 7, 1 mM $MgSO_4$ and 50 mM imidazole buffer, but the substrate concentration is unknown. Meyerhof and Oesper *(13)* determined $\Delta^R g'^0$ = -2.63 kJ mol^{-1} at 297.15 K in bicarbonate buffer with Mg^{2+} as a cofactor but unknown pH and unknown concentrations. A value generally recommended and often used in thermodynamic feasibility analyses for the enolase reaction was published by Garrett and Grisham: $\Delta^R g'^0$ = 1.8 kJ mol^{-1} determined at 298.15 K *(16)*. Another possible reason is the fact that authors did not convert their data to the standard state, e.g. to the hypothetically ideal solution. This means the values of $\Delta^R g'^0$ given by several authors might have been determined at different medium conditions and are thus not necessarily consistent standard data. To overcome this issue, in this work $\Delta^R g'^0$ was determined considering the influence on the measuring conditions by activity-based equilibrium constants. That required measuring equilibrium concentrations and predicting the corresponding activity coefficients of the reacting agents. The latter were predicted with the equation of state ePC-SAFT *(17,18)*. ePC-SAFT allows describing interactions between charged biomolecules by predicting activity coefficients in multi-component systems with a high

accuracy and reliability *(19–22)*. This procedure will allow for a correct thermodynamic characterization of the enolase reaction.

Thermodynamic Formalism for Enolase Reaction

The enzyme enolase converts D-2-phosphoglycerate (2-PG) to phosphoenolpyruvate (PEP) and water, see eq. (2)**Error! Reference source not found.**. Eq. (2)**Error! Reference source not found.** shows the textbook biochemical expression while eq. (3) shows the real chemical reaction.

$$\text{2-PG}^{3-} \rightleftharpoons \text{PEP}^{3-} + \text{H}_2\text{O} \qquad (3)$$

With the biochemical definition, the apparent equilibrium constant K'_m is defined as seen in eq. (4) based on the sum of species molalities. The sum of species molalities means the sum of the molalities of each single species of a substance (e.g. PEP is the sum of the molalities of the species H_3PEP, H_2PEP^-, $HPEP^{2-}$ and PEP^{3-}). With the chemical definition, K_m is defined as seen in eq. (5) based on the molalities of the reacting species *(23)*. Please note, that in literature, the apparent equilibrium constant of reactions including water as a reactant or product occurring in aqueous solutions, is often defined without $m_{\mathrm{H_2O}}^{eq}$. In this work, we introduce a generally applicable procedure. Thus, water will be considered and its activity will not be set to one, but will be calculated from $m_{\mathrm{H_2O}}^{eq}$ and the corresponding activity coefficient $\gamma_{\mathrm{H_2O}}^{m,eq}$, yielding a thermodynamically correct description of the enolase reaction. This means that literature values for the

apparent equilibrium constant, where water was not considered, need to be multiplied with $m_{\mathrm{H_2O}}^{eq}$. This is a factor of 55.51 mol kg^{-1}. In this work molalities were used as concentration scale. In contrast to molarity (mol/L) molality is a temperature-independent unit that does not depend on density of solution. It should be noted that molality and molarity are similar numbers given that the sum of concentration of all components (except water) is low.

$$K'_m = \frac{m_{\mathrm{PEP}}^{eq} \cdot m_{\mathrm{H_2O}}^{eq}}{m_{\mathrm{2\text{-}PG}}^{eq}} \tag{4}$$

$$K_m = \frac{m_{\mathrm{PEP^{3-}}}^{eq} \cdot m_{\mathrm{H_2O}}^{eq}}{m_{\mathrm{2\text{-}PG^{3-}}}^{eq}} \tag{5}$$

To calculate $\Delta^{\mathrm{R}}\mathrm{g}'^{0}$ from activities, activity coefficients of the reactants and products at equilibrium $\gamma_i^{m,eq}$ are required. These can be predicted with models such as equations of state or g^{E}-models. In this work, ePC-SAFT is used for this purpose. In order to account for the different species of the substances present in the reaction medium, activity coefficients were species-averaged (i.e. one activity coefficient was used to describe the different species of a substance). Two different types of activity coefficients were used: the generic activity coefficient γ_i, for which the standard state is the pure substance and the rational activity coefficient γ_i^*, for which the standard state is the hypothetical ideal solution. In this work we define hypothetical ideal solution as an infinite dilution of the substance in water. γ_i^* was calculated from γ_i with eq. (6), using the activity coefficient at infinite dilution γ_i^∞.

$$\gamma_i^* = \frac{\gamma_i}{\gamma_i^\infty} \tag{6}$$

As water is a product and the solvent of the enolase reaction at the same time (see eq. (2)**Error! Reference source not found.**) and thus, is closer to a standard state of pure substance, the generic activity coefficient on molality base $\gamma_{\mathrm{H_2O}}^{m}$ is used for water. For 2-PG and PEP, which are highly diluted in water, the rational activity coefficient on molality base $\gamma_i^{*,m}$ is used. Thus, K'_γ, the activity-coefficient ratio based on species-averaged activity coefficients, is expressed according to eq. (7).

$$K'_\gamma = \frac{\gamma_{\mathrm{PEP}}^{*,m,eq} \cdot \gamma_{\mathrm{H_2O}}^{m,eq}}{\gamma_{\text{2-PG}}^{*,m,eq}} \tag{7}$$

At the standard state “hypothetical ideal solution”, $\gamma_{\text{2-PG}}^{*,m}$ and $\gamma_{\mathrm{PEP}}^{*,m}$ are equal to one. $\gamma_{\mathrm{H_2O}}^{m}$ becomes $m_{\mathrm{H_2O}}^{-1}$ at the standard state “pure water”. This is due to eq. (8): for pure water, $\gamma_{\mathrm{H_2O}}^{x}$ is by definition equal to one. Thus, $a_{\mathrm{H_2O}}$ is equal to one and $\gamma_{\mathrm{H_2O}}^{m}$ is equal to $m_{\mathrm{H_2O}}^{-1}$, which is a value of 0.018015 kg mol^{-1}. That is, eq. (7) becomes eq. (9) in the ideal case.

$$a_{H_2O} = m_{H_2O} \cdot \gamma_{H_2O}^{m} = x_{H_2O} \cdot \gamma_{H_2O}^{x} \tag{8}$$

$$K_\gamma^{\prime,ideal} = \frac{\gamma_{PEP}^{*,m,ideal} \cdot \gamma_{H_2O}^{m,ideal}}{\gamma_{2-PG}^{*,m,ideal}} = \frac{1 \cdot 1/m_{H_2O}}{1} \tag{9}$$

The biochemical thermodynamic equilibrium constant K'_a is calculated with eq. (10) from K'_m and K'_γ. It is used to calculate $\Delta^R g'^0$ according to eq. (11).

$$K'_a = K'_m \cdot K'_\gamma = \frac{a_{\mathrm{PEP^{3-}}}^{eq} \cdot a_{\mathrm{H_2O}}^{eq}}{a_{\text{2-PG}^{3-}}^{eq}} \tag{10}$$

$$\Delta^R g'^0 = -RTln(K'_a) \tag{11}$$

The temperature dependency of K'_a was described by the standard enthalpy of reaction $\Delta^R h'^0$, which is shown by the van ’t Hoff equation in eq. (12).

$$\left(\frac{dlnK_a'}{dT}\right)_{\mathrm{p}} = \frac{\Delta^R h'^0}{\mathrm{RT}^2} \tag{12}$$

Integrating eq. (12) assuming a temperature-independent reaction enthalpy yields eq. (13).

$$ln\left(\frac{K_a'(T_2)}{K_a'(T_1)}\right) = -\frac{\Delta^R h'^0}{\mathrm{R}}\left(\frac{1}{T_2} - \frac{1}{T_1}\right) \tag{13}$$

Calculation of pH and pMg Dependency of Enolase Reaction

pH has an influence on the reaction equilibrium of biochemical reactions if one of the reacting agents is able to dissociate und thus, the concentration of the reactive species is modified by pH. The pH dependency of a reaction can be calculated given that the distribution of the differently charged species of the reactants and products at a certain pH is known. The species distribution can be calculated with the dissociation constants of the substances. The dissociation constants K_A are defined as shown in eq. (14). The molalities of the charged dissociated species $m(A^-)$, the non-dissociated species $\mathrm{m}(HA)$ and the activity of the hydrogen ion $a(\mathrm{H}^+)$ are required (see eqs. (S5)-(S7) in the SI (chapter 2.) for example).

$$K_{\mathrm{A}} = \frac{m(\mathrm{A}^-) \cdot a(\mathrm{H}^+)}{\mathrm{m(HA)}} \tag{14}$$

For these equations it is assumed that the species have the same activity coefficients; this assumption has shown to be acceptable for many biochemical reactions. Eq. (15) shows how the fraction of the non-dissociated species Λ_{HA} can be calculated in an aqueous solution, where the non-dissociated species and the dissociated species are present. Therefore, $\mathrm{K_A}$ and $a(\mathrm{H}^+)$ need to be known (see eq. (S8) in the SI for example).

$$\Lambda_{\mathrm{HA}} = \left(1 + \frac{K_{\mathrm{A}}}{a(\mathrm{H}^+)}\right)^{-1} \tag{15}$$

In order to account for complex formation with magnesium, complex dissociation constants K_{Mg} are needed, which are defined as shown in eq. (16) (see eqs. (S9)-(S10) in the SI for example).

$$K_{\mathrm{Mg}} = \frac{m(\mathrm{A}^{2-}) \cdot m(\mathrm{Mg}^{2+})}{m(\mathrm{MgA})} \tag{16}$$

The equation system, which is needed to calculate the Λ for the different species, was solved iteratively with the bisection method. This was necessary as $m(\mathrm{Mg}^{2+})$ depends on the Λ and is not known from a measurement (in contrast to $a(\mathrm{H}^+)$).

Figure 1 shows the calculated species distribution of PEP. The pK_A and pMg values for the calculation were taken from literature or were estimated and are listed in Table S1 in the SI. Figure 1 further shows that the $MgPEP^{1-}$ species is not present in the aqueous solutions used in this work. Thus, we did consider Mg^{2+} for all activity-coefficient calculations in this work but we did not consider the $MgPEP^{1-}$ species.

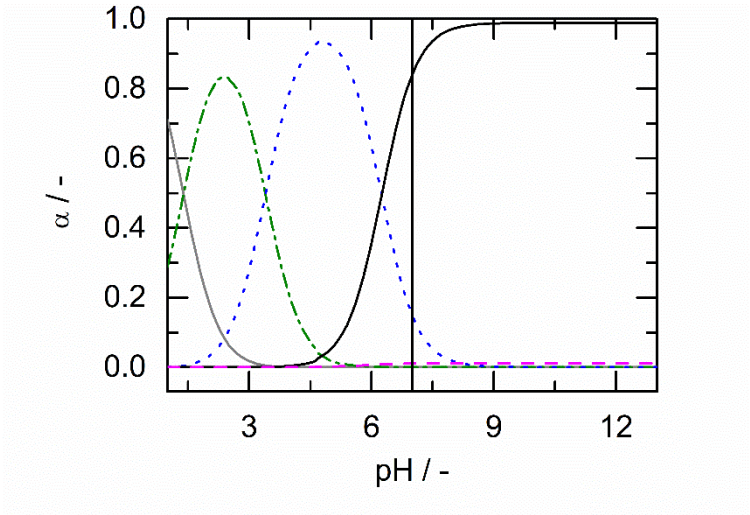

Figure 1: Species distribution of PEP: solid (black) line represents PEP^{3-}, dotted (blue) line represents $HPEP^{2-}$, dashed - dotted (green) line represents H_2PEP^-, gray solid line represents uncharged H_3PEP and dashed line (magenta) represents $MgPEP^{1-}$. pK_A and pMg values were taken from Table S1 (see SI). Calculation was performed for $m_{Mg^{2+}}$ = 0.8 mmol kg^{-1} and m_{PEP} = 13.4 mmol kg^{-1}. Vertical line indicates pH 7.

Materials and Methods

Materials

The substances used in this work are listed in Table S2 in the SI and have been used without further purification. The enzyme used in this work was a lyophilized enolase from *Saccharomyces cerevisiae*. According to the supplier, the enzyme should be prepared in a 15 mmol kg^{-1} Trizma™-hydrochloride solution and is activated by Mg^{2+}, which is why these conditions were used for the equilibrium measurements. Further, the enzymatic activity for different reactions was tested by the supplier with results of zero activity (0 U g^{-1}) for both, 3-phosphoglycerate kinase reaction and glyceraldehyde 3-phosphate dehydrogenase reaction. Another potentially overlapping reaction is the conversion of phosphoenolpyruvate and bicarbonate into oxaloacetate catalyzed by carboxylases. In

order to be able to exclude this side reaction, aspartate was added as a well investigated inhibitor of the carboxylation *(24)*. A significant contribution of the carboxylation can be excluded from the coincidence of the calorimetrically monitored reaction rates with and without inhibitor (Figure S1 in SI). This is important, as reactions occurring simultaneously to the enolase reaction, would influence the equilibrium measurements. The water used in this work was ultra-pure water freshly generated with a Millipore® purification system (Merck KGaA, Darmstadt, Germany). The water content of the phospho(enol)pyruvic acid monosodium salt hydrate, which was provided by the supplier, was considered in all calculations. All solutions were composed by weight with an analytical balance XS205 (Mettler Toledo GmbH, Gießen, Germany) with an accuracy of 0.01 mg.

Measurement of Densities and Osmotic Coefficients

In order to determine pure-component and binary interaction parameters required for the ePC-SAFT modeling, densities and osmotic coefficients of the system water and PEP were measured. Densities of aqueous PEP solutions with different concentrations were measured with a micro-viscometer Lovis 2000 M/ME, which is combined with the density meter DMA 4100 M (Anton Paar GmbH, Graz, Austria), maintained at 298.15 K. The measurement of osmotic coefficients were performed using a freezing point osmometer OSMOMAT 010 (Gonotec GmbH, Berlin, Germany), which was calibrated with aqueous sodium chloride standards provided by Gonotec. As described before, PEP dissociates in water yielding different PEP species with different charges. Thus, different pH values of the solution yield different osmotic coefficients. In order to account for this behavior, the pH values were adjusted with sodium hydroxide prior to the measurement of osmotic coefficients. Three different pH values 2.5, 5.1 and 8.2 were adjusted, each of them

corresponding to a maximum concentration of H_2PEP^-, $HPEP^{2-}$, PEP^{3-}, respectively. Afterwards, the measurement was performed and the osmotic coefficient ϕ was calculated with eq. (17) from the measured osmolality osm. Because of the addition of sodium hydroxide to the solution the ions stemming from this have also to be accounted for in the denominator of eq. (17).

$$\phi = \frac{osm}{m_{Na^+} + m_{OH^-} + m_{H^+} + m_{PEP}} \tag{17}$$

Where $\boldsymbol{m_{PEP}}$ means the sum of all PEP species. Please note, that $\boldsymbol{m_{OH^-}}$ was so low that it was neglected in the following.

Equilibrium Experiments

The experiments were carried out in 1.5 mL Eppendorf Tubes® (Eppendorf AG, Hamburg, Germany), which were placed in a ThermoMixer C (Eppendorf AG, Hamburg, Germany). In order to ensure that equilibrium was reached, the evolution of PEP concentration was measured over time in three separate reaction vessels. Equilibrium was defined as the time point where the concentration of PEP was constant. Prior to this, solutions containing the substances required for the reaction were freshly prepared by weighing: first, a buffer solution was made from 15 mmol kg^{-1} Trizma™-hydrochloride and 15 mmol kg^{-1} Trizma® base solutions, such that pH 7.0 was reached (measured with a QpH 70 by VWR International GmbH, Darmstadt, Germany). Afterwards, a buffer solution containing $MgCl_2$ was prepared by adding the buffer solution to solid $MgCl_2$. The enzyme enolase was weighed and diluted in the buffer solution containing $MgCl_2$. According to the supplier, this creates a suitable reaction medium for the enzyme. PEP was weighed and diluted in the buffer solution. Afterwards, these two solutions were mixed such that the desired reaction conditions were achieved. The reaction medium

thus contained 3-5 U g^{-1} enolase, which leads to a reaction time of <30 min until equilibrium was reached at the reaction conditions used in this work (validated for 298.15 K). The pH value was adjusted to 7.0 by adding NaOH; the amount of NaOH solution, which was added to the reaction medium was determined gravimetrically. The reaction was carried out at reaction temperature (298.15 K, 305.15 K or 310.15 K) and 350 rpm.

Concentration Analysis

The samples of the equilibrium experiments were analyzed in a UV spectrometer BioSpectrometer® kinetic (Eppendorf AG, Hamburg, Germany), which was maintained at reaction temperature (298.15 K, 305.15 K or 310.15 K ±0.1 K). A High Precision cuvette (Hellma Analytics, Müllheim, Germany) with a pathway of 10 mm was used. Prior to the UV measurements, a calibration curve of the UV absorption of PEP at 245 nm was determined for molalities between 0 and 3 mmol kg^{-1} PEP in 15 mmol kg^{-1} Tris buffer including 1 mmol kg^{-1} $MgCl_2$ at 298.15 K and pH 7. The coefficient of determination of the linear calibration curve, consisting of eight three-fold determinations, was 0.999. The molal extinction coefficient at 298.15 K is 695 kg mol^{-1} cm^{-1} (see Figure S2 in the SI). The blank for all measurements also consisted of 15 mmol kg^{-1} Tris buffer including 1 mmol kg^{-1} $MgCl_2$ at pH 7. The enolase did not show any significant influence on the UV measurements under all measuring conditions. All experiments with equilibrium molalities of PEP of > 3 mmol kg^{-1} required further treatment of the samples. These samples were separated from the enzyme by placing them in a Centrifuge 5418 R (Eppendorf AG, Hamburg, Germany) at 16 g at the same temperature as the reaction temperature. VWR centrifugal filters (VWR International GmbH, Darmstadt, Germany) with a pore size of 10 kDa were used (enolase has a

molecular weight of 90 kDa). Afterwards, the samples were diluted in 15 mmol kg^{-1} Tris buffer including 1 mmol kg^{-1} $MgCl_2$ in order to reach concentrations of PEP < 3 mmol kg^{-1}. The so-obtained dilutions were finally measured with the UV spectrometer at 245 nm. The equilibrium molality of 2-PG $m_{\text{2-PG}}^{eq}$ was calculated according to eq. (18) from the molality of PEP before the reaction $m_{\text{PEP}}^{t=0}$ and the molality of PEP at equilibrium m_{PEP}^{eq}.

$$m_{\text{2-PG}}^{eq} = m_{\text{PEP}}^{t=0} - m_{\text{PEP}}^{eq} \tag{18}$$

Thermodynamic Modeling

As shown in eqs. (10) and (11), activity coefficients are required for the calculation of $\Delta^R g'^0$ from experimental molalities. In this work, the equation of state ePC-SAFT, as proposed by Held et al. *(17)*, was used to predict activity coefficients. ePC-SAFT is based on original PC-SAFT from Gross and Sadowski *(18)* and the extension from Cameretti et al. *(25)*. Within ePC-SAFT, the residual Helmholtz energy A^{res} is calculated from different contributions, as shown in eq. (19).

$$A^{res} = A^{hc} + A^{disp} + A^{assoc} + A^{ion} \tag{19}$$

A^{hc} is the reference contribution which is calculated assuming a reference system of a hard chain composed of hard spheres. The other contributions account for perturbations to this hard sphere reference system. A^{disp} accounts for molecular dispersive interactions, which are related to the van der Waals energy. A^{assoc} accounts for associative interactions such as hydrogen bonding forces and A^{ion} accounts for Coulomb interactions, described by a Debye-Hückel expression. In order to account for these contributions, five pure-component parameters are required for ePC-SAFT. The geometry of the hard sphere reference system is described by the segment number m_i^{seg} and the segment diameter σ_i. Dispersive interactions are described by the

dispersion-energy parameter u_i/k_B including the Boltzmann constant k_B. Associative interactions are described by the association-energy parameter $\varepsilon^{A_iB_i}/k_B$ and the association-volume parameter $\kappa^{A_iB_i}$. Additionally, the number of association sites N_i^{assoc} has to be chosen prior to modeling.

Based on mixing rules (see eqs. (S1)-(S4) in the SI, chapter 1.) the residual Helmholtz energy A^{res} is expressed for any multi-component mixture. Derivation of A^{res} with respect to density and mole fraction yields fugacity coefficients and activity coefficients of the reactants and products (standard procedures according to *(26)*).

Estimation of ePC-SAFT Parameters

As described before, five pure-component parameters and one binary interaction parameter between a substance and water and between ions are required for the thermodynamic modeling with ePC-SAFT. The parameters for water, the ions Na^+, Mg^{2+} and Cl^- and the buffer component Tris base were available from literature (Table 1). The pure-component parameters for the buffer component Tris-H^+ were also available from literature, but the binary interaction parameter between water and Tris-H^+ had to be fitted in this work to experimental osmotic coefficients at 298.15 K available from literature *(27)*. The ePC-SAFT parameters for PEP were fitted to osmotic coefficients from own measurements. 2-PG was not available for purchase. Thus, the 2-PG parameters were inherited from the isomer 3-PG, which is a reasonable assumption and even more, the 3-PG parameters were available from literature *(9)*. Therefore, the following objective function OF was minimized using a Levenberg-Marquardt algorithm for the number of experimental data points NP.

$$\mathrm{OF} = \sum_{k=1}^{NP(\phi)} \left| 1 - \left(\frac{\phi^{mod}}{\phi^{exp}} \right)_k \right| + \sum_{m=1}^{NP(\rho)} \left| 1 - \left(\frac{\rho^{mod}}{\rho^{exp}} \right)_m \right| \tag{20}$$

The resulting pure-component and the binary interaction parameters estimated in this work, as well as the applied parameters available from literature are listed in Table 1.

Table 1: ePC-SAFT parameters applied in this work with the sources for the respective sets of parameters. For 2-PG the parameters of its isomer 3-PG were used.

	m_i^{seg}	σ_i	u_i/k_B	N_i^{assoc}	$\varepsilon^{A_iB_i}/k_B$	$\kappa^{A_iB_i}$	k_{i,H_2O}	q	source
	-	Å	K	-	K	-	-	-	
PEP	12.007	2.200	407.27	2+2	5000	0.1	[a]	-2	
3-PG or 2-PG	3.110	4.66	322.02	5+5	501.2	10^{-4}	[b]	-2	*(9)*
Tris	6.373	2.748	302.16	1+1	4786.9	0.020271	-0.047	-	*(5)*
Tris-H^+	10.205	2.408	348.10	4+4	10970.9	10^{-6}	-0.061[c]	-	*(5)*
water	1.2047	[d]	353.94	1+1	2425.7	0.045099	-	-	*(28)*
Na^+ [e]	1	2.8232	230.00	-	-	-	[f]	+1	*(17)*
Mg^{2+} [g]	1	3.1327	1500.00	-	-	-	-0.25	+2	*(17)*
Cl^-	1	2.7560	170.00	-	-	-	-0.25	-1	*(17)*

[a] $k_{PEP,water}$ = -0.005083 T/K + 1.3316 (from this work)

[b] $k_{3-PG,water}$ = 0.002033 T/K – 0.7064 *(9)*

[c] $k_{Tris-H^+,water}$ (from this work)

[d] σ_{water} = 2.7927 + 10.11 exp(-0.01775 T/K) – 1.417 exp(-0.01146 T/K) *(28)*

[e] k_{Na^+,Cl^-} = 0.3166 *(17)*

[f] $k_{Na+,water}$ = -0.007981 T/K + 2.3799 *(17)*

[g] k_{Mg^{2+},Cl^-} = 0.817 *(17)*

Quantum-chemical calculations

Enthalpies of formation of model compounds were calculated with the composite G4 method implemented in the Gaussian 09 program package *(29)*. An initial search for the stable conformers was performed with the force field method MM3 *(30)* and the b3lyp/6-31g(d,p) method *(31)*. Energies E_0 and enthalpies H_{298} of the most stable conformers were calculated by using the composite method G4 *(32)* from the Gaussian 09 suit of programs. Details on computational procedure were reported elsewhere *(33)*. We used the values of H_{298} directly available from the output, which were obtained according to the “rigid rotator”-“harmonic oscillator” approach embedded in the Gaussian 09.

Results

Osmotic coefficients

The osmotic coefficients of the system water and NaPEP and the system water and Tris-HCl and the densities of the system water and NaPEP were used for fitting the pure-component parameters of PEP and Tris-H^+ and the binary parameters between these components and water. The results of the experimental osmotic coefficients of the system water and NaPEP and the resulting modeling curve from ePC-SAFT for the species $HPEP^{2-}$ are shown in Figure 2a and in Tables S3-S5 in the SI. The experiments show that the different PEP species interact differently with water, yielding different osmotic coefficients. This is mainly caused by the different charges of the PEP species. Figure 2a further shows that the difference between the species $HPEP^{2-}$ and PEP^{3-} is smaller than the difference between H_2PEP^- and $HPEP^{2-}$. The modeling with ePC-SAFT was performed using parameters for the species $HPEP^{2-}$, because $HPEP^{2-}$ and PEP^{3-},

which are mainly present at the investigated pH value of 7, show a similar behavior in aqueous solution. The results of the experimental densities of the system water and NaPEP and the resulting modeling curve from ePC-SAFT are shown in Figure 2c and Table S6 in the SI.

The experimental osmotic coefficients of the system water and Tris-HCl from Robinson and Bower *(27)* and the resulting modeling curve from ePC-SAFT are shown in Figure 2b. The good overall modeling results prove that the pure-component parameters of Tris-H^+ are still valid independent of the fact that the parameters were originally fitted by Hoffmann et al. *(5)* using outdated Cl^- parameters.

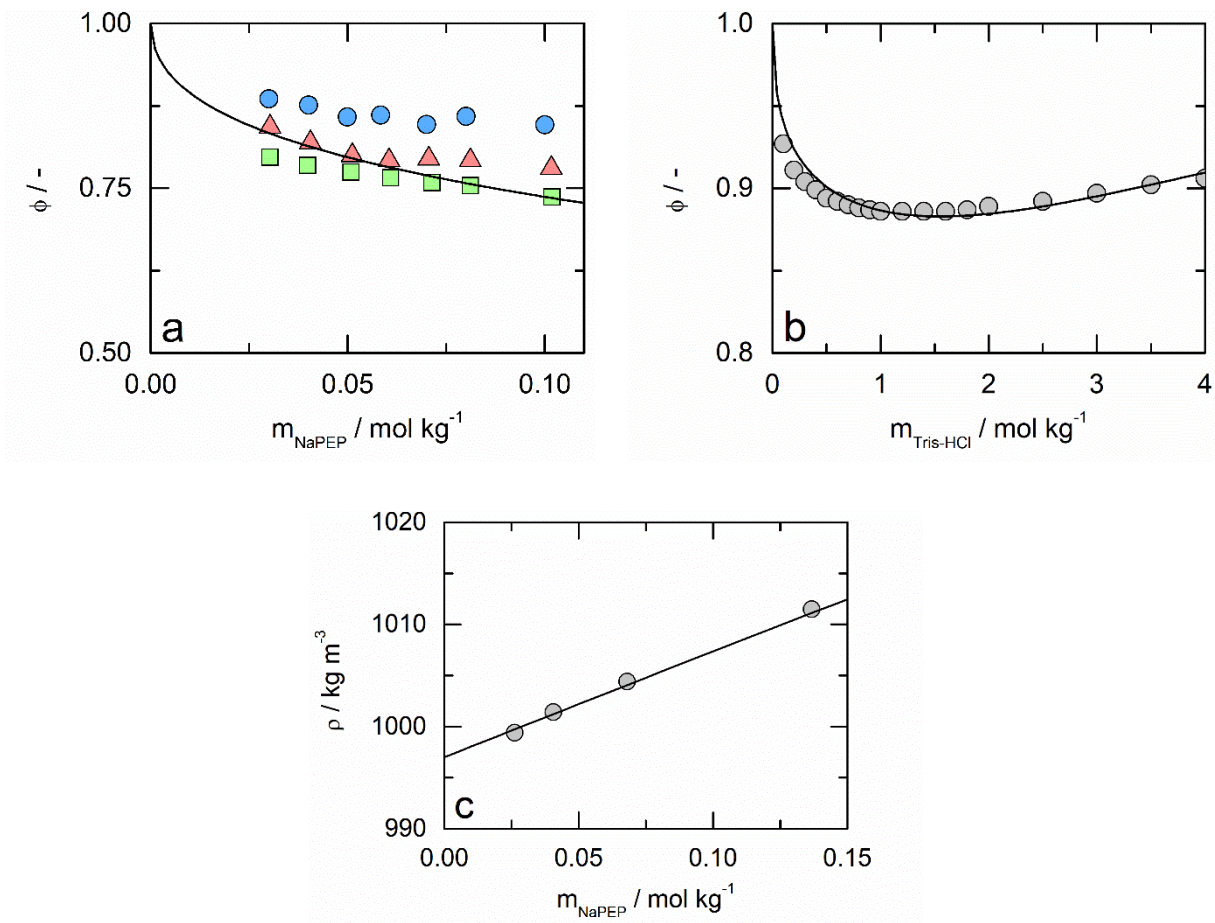

Figure 2: a: Osmotic coefficient ϕ vs molality of NaPEP m_{NaPEP} of aqueous NaPEP solutions at 273.15 K and 1 bar. Circles represent experimental data for the species H_2PEP^-, triangles represent experimental

data for the species $HPEP^{2-}$, squares represent experimental data for the species PEP^{3-}, solid line represents modeling with ePC-SAFT for the species $HPEP^{2-}$. **b:** Osmotic coefficient ϕ vs molality of Tris-HCl $m_{Tris-HCl}$ of aqueous Tris-HCl solutions at 298.15 K and 1 bar. Circles represent experimental data from Robinson and Bower *(27)*, solid line represents modeling with ePC-SAFT for Tris-H^+. Modeling using parameters from Table 1. **c:** Density ρ vs molality of NaPEP m_{NaPEP} of aqueous NaPEP solutions at 298.15 K and 1 bar. Circles represent experimental data, solid line represents modeling with ePC-SAFT for PEP using parameters from Table 1.

Standard Gibbs Energy of Reaction

The biochemical apparent equilibrium constant, expressed as K'_m, of the enolase reaction was calculated with eq. (4) using experimental equilibrium molalities of the reactants and products at 298.15 K, 1 mmol kg^{-1} Mg^{2+} and pH 7. The results in Figure 3a show that the reaction equilibrium does not significantly depend on the substrate molality. A slight increase of K'_m (about 10%) can be observed in the considered range from zero up to 13.5 mmol kg^{-1} PEP. Error bars in Figure 3 and all following figures as well as estimated uncertainties in Tables show the precision of the measurements and are estimated by means of a Taylor series using uncertainty stemming from triplet single measurements.

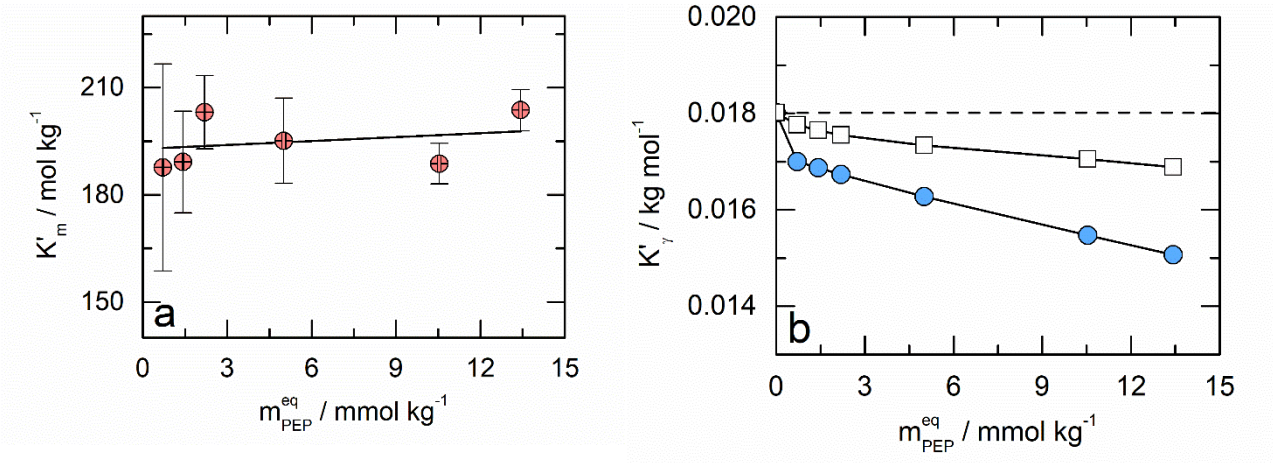

Figure 3: a: Apparent equilibrium constant on molality base K'_m vs equilibrium molality of PEP m_{PEP}^{eq} at 298.15 K, m_{MgCl_2} = 1 mmol kg^{-1}, m_{Tris} = 15 mmol kg^{-1}, pH 7 and 1 bar. Circles represent experimental data from this work, solid line represents linear fit to the experimental data. **b:** Activity-coefficient ratio K'_γ vs equilibrium molality of PEP m_{PEP}^{eq} at 298.15 K, m_{MgCl_2} = 1 mmol kg^{-1}, m_{Tris} = 15 mmol kg^{-1}, pH 7 and 1 bar. Circles represent predicted activity-coefficient ratio with ePC-SAFT, squares represent activity-coefficient ratio calculated with Debye-Hückel limiting law according to *(1)*, dashed line represents ideal value of $K'_\gamma(m_{PEP}$ = 0) = 0.01805 kg mol^{-1}.

In order to calculate the biochemical thermodynamic equilibrium constant K'_a, the activity-coefficient ratio K'_γ is required. K'_γ was calculated using the activity coefficients of the reactants and products with eq. (7). The activity coefficients were predicted with ePC-SAFT at the same conditions at which the equilibrium measurements were performed. For these predictions, all substances, which were present in the multi-component reaction medium during the equilibrium measurements, except the enzyme, have been considered explicitly. These included the reactants water and PEP, the product 2-PG, as well as the inert substances Mg^{2+}, Cl^-, Na^+ and the Trizma™-hydrochloride buffer which includes Tris-H^+ and the Tris base. The pure-component and binary interaction parameters, which are required for these predictions are listed in Table

1. Figure 3b shows the prediction results of the activity-coefficient ratio K'_γ together with the ideal value $K'^{,ideal}_\gamma$, which is 0.01805 kg mol^{-1} (see eq. (9) for explanation).

In contrast to the behavior of an ideal solution, ePC-SAFT predicts decreasing K'_γ with increasing molality of PEP. This is in accurate agreement with the increase of K'_m and proves a concentration-independent value for the thermodynamic equilibrium constant K'_a(298.15 K, pH 7) of 3.2±0.2. Based on this K'_a, the standard Gibbs energy of reaction $\Delta^R g'^0$ was calculated for different conditions under investigation using eq. (11). As shown in Figure 4, the calculation yields an average value of $\Delta^R g'^0$(298.15 K, pH 7) = -2.8±0.2 kJ mol^{-1}. Furthermore, the activity-coefficient ratio K'_γ determined with ePC-SAFT was compared to the determination with the Debye-Hückel limiting law in Figure 3b. The K'_γ values determined with ePC-SAFT are lower and differ more from the ideal value than the values determined with the Debye-Hückel limiting law, but both yield a decreasing K'_γ with an increasing molality of PEP at the reaction conditions used in this work.

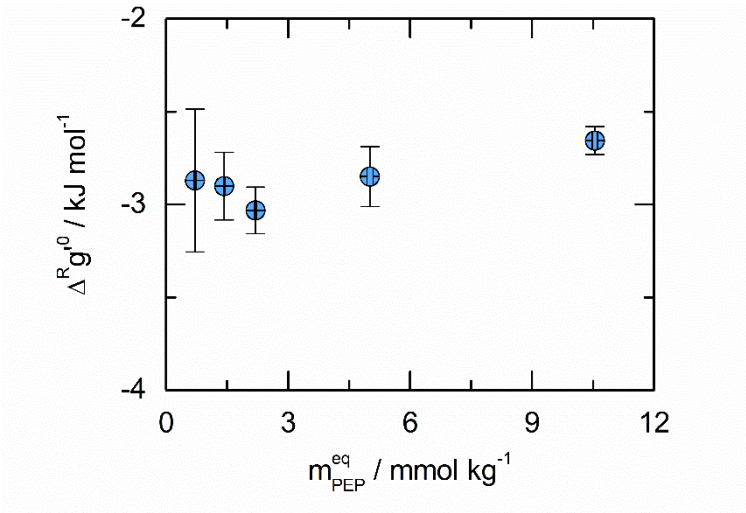

Figure 4: Standard Gibbs energy of biochemical reaction $\Delta^R g'^0$(298.15 K, pH 7) vs equilibrium molality of PEP m^{eq}_{PEP} at m_{MgCl_2} = 1 mmol kg^{-1}, m_{Tris} = 15 mmol kg^{-1} and 1 bar.

Influence of pH and pMg on reaction equilibrium

As previously described, pH might have a large influence on the equilibrium of many biochemical reactions. In general, pH influence can be calculated using dissociation constants K_{Ai} of the reactants and products. In order to apply this to the enolase reaction, the species distributions of 2-PG and PEP were calculated, as shown for PEP in Figure 1. The pK_{Ai} and pMg_i values for the calculation were taken from literature or were estimated and are listed in Table S1 in the SI. All measurements in this work were performed at pH 7.0±0.1, at which the reacting species PEP^{3-} is mainly present besides small amounts of the species $HPEP^{2-}$ and very small amounts of the complex $MgPEP^{1-}$. The pH-dependency of K'_m of the enolase reaction is shown in Figure 5. An increase of pH yields a significant increase of K'_m, i.e. the reaction equilibrium is shifted to the product side. The influence of pH on K'_m is strong in the range between pH 6 and pH 8, while the influence of pH on K'_m is comparably weak at pH < 5 and pH > 9. In the

interesting range for living systems between 5 and 9, K'_m is between 70 mol kg^{-1} and 300 mol kg^{-1}. For the sake of completeness, the value for the chemical apparent equilibrium constant K_m, which is a pH-independent value, is 314 mol kg^{-1} (see eq. (5) and reference *(7)* for the definition and the proof of a pH-independent K_m value).

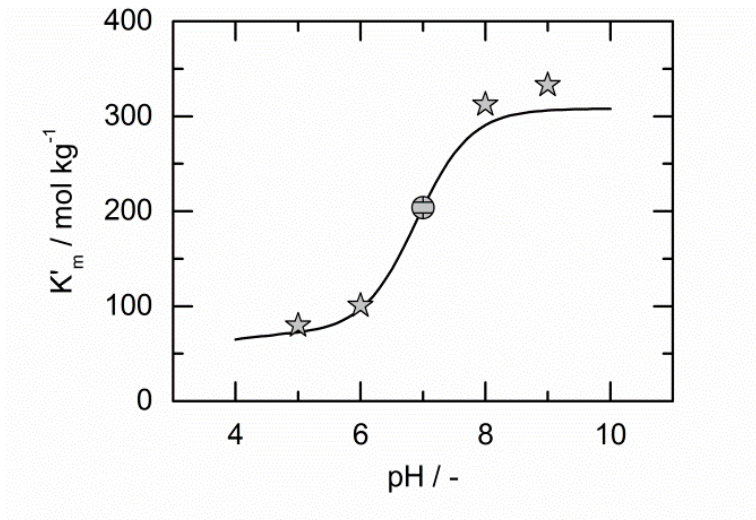

Figure 5: Biochemical apparent equilibrium constant on molality base K'_m vs pH at 298.15 K and 1 bar. Circle represents K'_m value from this work, stars represent data from Alberty *(12)* and solid line represents calculation based on species distribution. Calculation was performed for $m_{Mg^{2+}}$ = 1 mmol kg^{-1}, m_{2-PG} = 3.7 mmol kg^{-1} and m_{PEP} = 13.4 mmol kg^{-1} based on pK_{Ai} and pMg_i values from Table S1 (see SI).

Standard Enthalpy of Reaction

In order to determine the standard enthalpy of reaction $\Delta^R h'^0$ at 298.15 K and pH 7, the equilibrium constant K'_a was determined at different temperatures of 298.15 K, 305.15 K and 310.15 K. According to eq. (13), a linear regression in the van ’t Hoff plot was performed as shown in Figure 6. This procedure has been used in previous works and yields reliable $\Delta^R h'^0$ values that are consistent with other methods *(5,9,20,22)*. This yields a $\Delta^R h'^0$(298.15 K, pH 7) = 27±10 kJ mol^{-1}. The error represents the precision and

results from the errors of the measurements at the different temperatures, which allow different slopes in the van 't Hoff plot. A positive value means that the enolase reaction is endothermic and the equilibrium constant K'_a is favored by higher temperatures.

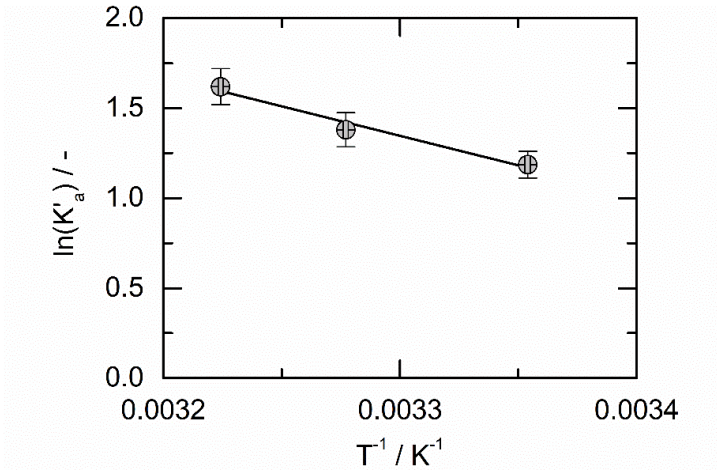

Figure 6: Natural logarithm of biochemical equilibrium constant K'_a vs inverse temperature at pH 7 and 1 bar. Line: linear regression to determine $\Delta^R h'^0$ with van 't Hoff equation.

Table 2: Biochemical apparent equilibrium constant on molality base K'_m calculated according to eq. (4) at experimental conditions (columns 1-3 and m_{Tris} = 15 mmol kg^{-1}, m_{MgCl_2} = 1 mmol kg^{-1}, pH 7 and 1 bar), biochemical activity-coefficient ratio K'_γ, biochemical equilibrium constant K'_a and biochemical standard Gibbs energy of reaction $\Delta^R g'^0$. Estimated errors provided in this table represent the precision of the measurements.

T	m^{eq}_{PEP}	$m^{eq}_{\text{2-PG}}$	K'_m	K'_γ	K'_a	$\Delta^{\text{R}} g'^0$
K	mmol kg^{-1}	mmol kg^{-1}	mol kg^{-1}	kg mol^{-1}	-	kJ mol^{-1}
298.15	0.71±0.02	0.21±0.03	188±29	0.0170	3.19±0.49	-2.87±0.38
298.15	1.43±0.02	0.42±0.03	189±14	0.0169	3.27±0.24	-2.94±0.18
298.15	2.20±0.02	0.60±0.03	203±10	0.0167	3.40±0.17	-3.03±0.13
298.15	5.01±0.07	1.44±0.08	195±12	0.0163	3.17±0.19	-2.85±0.16

298.15	10.54±0.06	3.10±0.08	189±6	0.0155	2.92±0.09	-2.66±0.08
298.15	13.43±0.06	3.66±0.09	204±6	0.0151	3.07±0.09	-2.78±0.07
305.15	1.54±0.02	0.36±0.02	233±22	0.0171	4.04±0.38	-3.54±0.24
310.15	1.60±0.01	0.30±0.02	294±29	0.0172	5.04±0.50	-4.17±0.25

Discussion

In this work, $\Delta^R g'^0$ was calculated from the activity-based thermodynamic equilibrium constant K'_a and thus, the $\Delta^R g'^0$-value is independent of initial substrate concentration at 298.15 K and pH 7 even if buffer or other inert species are present in the reaction mixture. In contrast, literature Gibbs energy of reaction values for the enolase reaction were calculated from the apparent equilibrium constant K'_m, see eq. (21). Thus, the literature values are only valid at the conditions at which the equilibrium concentrations were measured and they should be called '*observed standard Gibbs energy of reaction*' $\Delta^R g'^{0,obs}$.

$$\Delta^R g'^{0,obs} = -RTln(K'_m) \tag{21}$$

These data are – in contrast to values based on our K'_a – neither valid at other concentrations nor if other inert species or buffer components are present. Even worse, such inconsistent data have been used in current thermodynamic feasibility analyses. Available $\Delta^R g'^{0,obs}$ values published for the enolase reaction are shown in Figure 7. Wold and Ballou *(15)* found a $\Delta^R g'^{0,obs}$(298.15 K, pH 7, 1 mM $MgSO_4$, 50 mM imidazole buffer, substrate concentration unknown) of -3.61 kJ mol^{-1}, while Meyerhof and Oesper *(13)* found an apparent equilibrium constant of 2.9$\cdot m_{H_2O}$, which yields a $\Delta^R g'^{0,obs}$(297.15 K, pH unknown, concentrations unknown) of -2.63 kJ mol^{-1}. Both values

are in the same order of magnitude as the $\Delta^R g'^{0,obs}$(298.15 K, pH 7, 1.4 mM PEP, 0.4 mM 2-PG, 15 mM Tris buffer, 1 mM $MgCl_2$) of -3.1±0.2 kJ mol^{-1} found in this work. However, as the conditions (concentration, ions, buffer components and strength) were probably different, the qualitative agreement of these different values are mere chance. Wold and Ballou *(15)* investigated the enolase reaction at different concentrations of $MgSO_4$ (0 – 0.01 mol dm^{-3}), $MnSO_4$ (0 – 5 mmol dm^{-3}) and KCl (0 – 0.4 mol dm^{-3}), at different temperatures (288 – 307.5 K) and at different pH values (5.9 – 8.5). They performed the reaction in 0.05 mol dm^{-3} imidazole buffer. The $\Delta^R g'^{0,obs}$(298.15 K, pH 7,) value of -3.61 kJ mol^{-1} is calculated from an apparent equilibrium constant measured with 1 mmol dm^{-3} $MgSO_4$ and 0.05 mol dm^{-3} imidazole buffer. The equilibrium or starting concentrations of the substrates are unknown; thus, unfortunately, the $\Delta^R g'^{0,obs}$ cannot be converted into $\Delta^R g'^0$ by using activity coefficients. Meyerhof and Oesper *(13)* performed the enolase reaction and the phosphoglyceric mutase reaction simultaneously and calculated the apparent equilibrium constant of the enolase reaction from the overall apparent equilibrium constant of both reactions. They performed the reaction at 297 K and the $\Delta^R g'^{0,obs}$(298.15 K, pH unknown, concentrations unknown), transformed with the $\Delta^R h'^0$(298.15 K, pH 7) from this work (value of 27±10 kJ mol^{-1}), is -2.73 kJ mol^{-1}. They performed the reaction in bicarbonate buffer and used Mg^{2+} as a cofactor. However, it is unknown at which pH the reaction was performed, which means that this value should not be used for any calculations and should not be compared to other values, since pH has a large influence on the enolase reaction. Burton and Krebs *(2)* calculated a $\Delta^R g'^0$(298.15 K, pH 7) of -0.15 kJ mol^{-1}. Warburg and Christian *(14)* found a $\Delta^R g'^{0,obs}$(293.15 K, pH 7.34, 50 mM bicarbonate buffer, 30 mM glycine, 3 mM $MgSO_4$, 0.9 mM PEP, 2.1 mM 2-PG) of -0.87 kJ mol^{-1}. This value was transformed in the

present work to pH 7 and 298.15 K with $\Delta^R h'^0$(298.15 K, pH 7) = 27 kJ mol^{-1} and the species distribution yielding $\Delta^R g'^{0,obs}$(298.15 K, pH 7, 50 mM bicarbonate buffer, 30 mM glycine, 3 mM $MgSO_4$, 0.9 mM PEP, 2.1 mM 2-PG) = -0.89 kJ mol^{-1}. Further, Warburg and Christian performed the equilibrium measurements at non-ideal medium compositions (0.05 mol dm^{-3} bicarbonate, 0.03 mol dm^{-3} glycine and 3 mmol dm^{-3} $MgSO_4$, initial concentration of sodium D-2-PG was 1.5 mmol dm^{-3} stemming from a 3 mmol dm^{-3} racemic mixture). Thus, in the present work the activity coefficients of water, 2-PG and PEP were predicted with ePC-SAFT and $\Delta^R g'^{0,obs}$(298.15 K, pH 7, 50 mM bicarbonate buffer, 30 mM glycine, 3 mM $MgSO_4$, 0.9 mM PEP, 2.1 mM 2-PG) was transformed into $\Delta^R g'^0$(298.15 K, pH 7) finally yielding a value of -0.91 kJ mol^{-1}. This value still differs significantly from the value found in this work ($\Delta^R g'^0$(298.15 K, pH 7) = -2.8±0.2 kJ mol^{-1}). For an exact comparison, uncertainty of data from Warburg and Christian would be required.

Values which are generally recommended and often used in thermodynamic feasibility analyses for the enolase reaction were published by Garrett and Grisham, i.e. $\Delta^R g'^{0,obs}$(298.15 K, pH unknown, concentrations unknown) of 1.8 kJ mol^{-1} *(16)*. The value is assumed to be the same at 298 K and 310 K and the pH value is even unknown. Especially this value should not be used to perform a thermodynamic feasibility analysis. The fact that this value is positive means that the equilibrium at the conditions where the measurement was performed was on the side of the reactant 2-PG. In contrast, all other literature values, which are presented in Figure 7, found that the equilibrium was on the side of PEP at pH 7 and 298.15 K. According to the species distribution from this work, even at pH 4, the concentration of the product PEP is slightly

higher than the concentration of the reactant 2-PG. Thus, it is unclear how the positive $\Delta^R g'^{0,obs}$ value was determined.

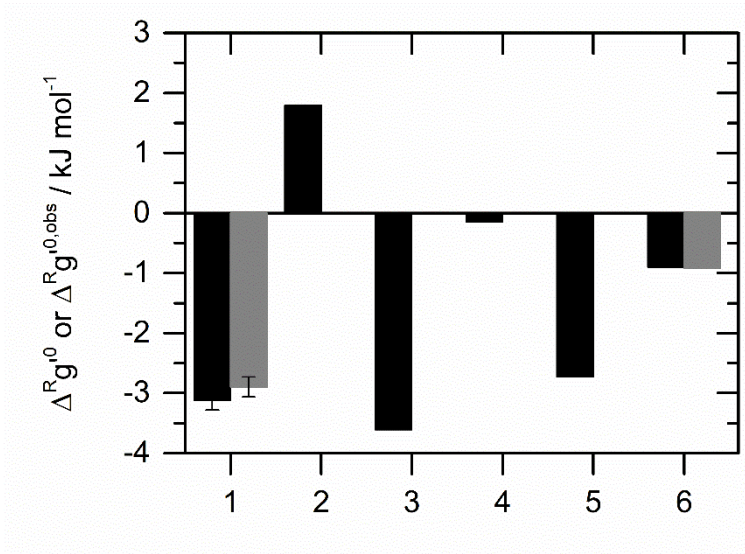

Figure 7: Gray bars represent $\Delta^R g'^0$(298.15 K, pH 7) $(= -RTln(K'_a))$ and black bars represent $\Delta^R g'^{0,obs}$(298.15 K, pH 7) $(= -RTln(K'_m \cdot K'^{ideal}_\gamma)$ with $K'^{ideal}_\gamma = m^{-1}_{H_2O})$. 1: own values, 2: Garrett and Grisham *(16)*, 3: Wold and Ballou *(15)*, 4: Burton and Krebs *(2)*, 5: Meyerhof and Oesper *(13)* corrected for temperature with $\Delta^R h'^0$(298.15 K, pH 7) from this work, 6: Warburg and Christian *(14)* corrected for temperature and pH with $\Delta^R h'^0$(298.15 K, pH 7) and the species distribution from this work (black) and combined with activity coefficients predicted with ePC-SAFT (gray).

The equilibrium of the enolase reaction is influenced significantly by pH as shown in Figure 5, because the reactant 2-PG and the product PEP dissociate in water and only one of the respective dissociated species is converted by the enzyme (see eq. (3)). As shown in Figure 5, especially at pH values about 7, the equilibrium is strongly pH-dependent. It is recommended to exactly measure pH while performing equilibrium measurements of the enolase reaction and to specify at which pH the equilibrium was measured when publishing K'_m values.

Standard enthalpy of reaction for different scales

As mentioned above, the value for $\Delta^R g'^{0,obs}$ is assumed to be the same at 298 K and 310 K in thermodynamic feasibility analyses for the enolase reaction as recommended in the literature *(16)*. That is, $\Delta^R h'^0$ is postulated to be zero. However, the standard enthalpy of reaction $\Delta^R h'^0$(298.15 K, pH 7) of 27±10 kJ mol^{-1} as determined in this work indicates that the enolase reaction is an endothermic reaction. This was also found by Wold and Ballou *(15)*, who found a $\Delta^R h'^{obs}$(298.15 K, pH 7.5, 8 mM $MgSO_4$, 0.4 M KCl, substrate concentrations unknown) of 15 kJ mol^{-1}. Our value and that from Wold and Ballou (derived from equilibrium measurements and the van 't Hoff equation) were determined at different pH values, which potentially explains the difference between both values. Furthermore, Wold and Ballou did not provide any error estimation, which complicates the data comparison. In general, it is known from chemical dehydration reactions that these are rather exothermic (e.g. Figure S6 in the SI). In the following, we suggest an explanation of the strong endothermic behavior we found in this work. To this end, standard data can also be accessed by means of quantum chemistry even at different scale. The enzymatically catalyzed dehydration reaction of D-2-phosphoglycerate (2-PG) to phosphoenolpyruvate (PEP) according to eq. (2)**Error! Reference source not found.** studied in this work was further addressed by quantum-chemical (QC) methods to assess energetics of biologically relevant reactions. It is well established that the high-level QC-methods (e.g. the composite method G4) are able to provide reliable gas-phase enthalpies of formation $\Delta^g h^0$ (298.15 K) at the level of "chemical accuracy" of 2 – 4 kJ mol^{-1} *(34)*. Thus, the reaction enthalpies of any reaction

in the gas phase can be calculated according to the Hess´s Law. However, the biological reactions proceed mostly in aqueous medium and a direct propagation of gas-phase QC-results to these conditions seems to be overoptimistic. In order to overcome this difficulty, we are developing a concept based on a “model molecule” (see Figure S3 in the SI) in this work. For example, for 2-PG we suggest to cut the PO_3^{2-} fragment and to attach the CH_3 group instead. Moreover, in order to avoid any charge of the model molecule we attached a proton to the (O=C-O$^-$)-group. The resulting model molecule is the 3-hydroxy-2-methoxy propionic acid. This model contains all specific characteristics for 2-PG groups, but it is not charged and its gas-phase enthalpy of formation $\Delta^g h^0$ (298.15 K) = -740.9 kJ mol^{-1} was calculated by the G4-method. In the same way we have “re-shaped” (see Figure S3 in the SI) the PEP and the enthalpy of formation $\Delta^g h^0$ (298.15 K) = -461.8 kJ mol^{-1} of the model molecule 2-methoxy acrylic acid was calculated. In order to get the required thermochemical property in the liquid phase we calculated standard molar vaporization enthalpies $\Delta_l^g h^0$ (298.15 K) = 98.0 kJ mol^{-1} for 3-hydroxy-2-methoxy propionic acid and $\Delta_l^g h^0$ (298.15 K) = 65.1 kJ mol^{-1} for 2-methoxy acrylic acid. Calculations of vaporization enthalpies have been performed by using well-established group-additivity procedure with uncertainty assessed to be of 1.5 kJ mol^{-1} *(35)*. Combination of $\Delta^g h^0$ (298.15 K) and $\Delta_l^g h^0$ (298.15 K)-values lead to the standard molar liquid-phase enthalpies of formation $\Delta^l h^0$ (298.15 K) required for the calculation of the reaction enthalpy of the model reaction given in Figure S5 in the SI. Using the liquid-phase enthalpy of formation $\Delta^l h^0$ (298.15 K) = -285.8 kJ mol^{-1} *(36)* for water, the standard enthalpy of the model reaction (see Figure S5 in the SI) $\Delta^R h^0$(298.15 K) = 27±5 kJ mol^{-1} was estimated (uncertainty of vaporization enthalpies are included).

Please note, that this enthalpy has the standard state “pure component” in the liquid phase for water, 2-PG and PEP. All values determined in this work except QC methods have the standard state “hypothetical ideal solution” for 2-PG and PEP. However, the standard enthalpy of the model reaction (Figure S5 in the SI) is very similar to the result $\Delta^R h'^0$(298.15 K, pH 7) = 27±10 kJ mol^{-1} from van’t Hoff (Figure 6). Nevertheless, the endothermic effect of the 2-PG dehydration reactions derived experimentally and confirmed theoretically seems to be somewhat perplexing, because, e.g. the liquid-phase dehydration of ethanol is a highly exothermic process (Figure S6 in the SI). In order to get more insight in energetics of dehydration reactions, we collected thermochemical data for 1,2-ethanediol, 3-hydroxy-propionic acid and products of their dehydration (see Table S6 in the SI). It has turned out, that already for 1,2-ethandiol the sign of the reaction enthalpy is changed from negative to positive. Moreover, the reaction enthalpy of 3-hydroxy-propionic acid (which structurally is closest to the 2-PG) dehydration of 29±4 kJ mol^{-1} is in the same order of magnitude as observed already in the van ’t Hoff plot (27±10 kJ mol^{-1}, Figure 6).

In order to further prove the modeling approach developed in this work, the isomerization reaction (see eq. (22)) of D-3-phosphoglycerate (3-PG) to D-2-phosphoglycerate (2-PG) was additionally studied.

$$\text{3-PG} \rightleftharpoons \text{2-PG} \qquad (22)$$

The model for the 3-PG compound was “constructed” in the same way as it was made for 2-PG (see Figure S4 in the SI). The structure of the resulting model molecule 2-hydroxy-3-methoxy-propionic acid was optimized and calculated with the G4 method. The standard molar enthalpy of formation $\Delta^g h^0$ (298.15 K) = -746.5 kJ mol^{-1} and

standard molar vaporization enthalpy $\Delta_l^g h^0$ (298.15 K) = 94.7 kJ mol^{-1} were used to estimate the liquid-phase enthalpy of formation $\Delta^l h^0$ (298.15 K) = -841.2 kJ mol^{-1} for 2-hydroxy-3-methoxy propionic acid. The latter value was used to calculate the theoretical reaction enthalpy $\Delta^R h^0$(298.15 K) = 2±5 kJ mol^{-1}, according to eq. (22). The small value of the enthalpy met reasonable expectations for such type of isomerization reactions.

To sum up, we calculated the enthalpy of reaction with the standard state "pure-component" to be $\Delta^R h^0$(298.15 K) = 27±5 kJ mol^{-1} based on QC methods. Additionally, we determined the enthalpy of reaction with standard state "hypothetical ideal solution" from equilibrium measurements at 298.15 – 310.15 K using the van 't Hoff equation to be $\Delta^R h'^0$(298.15 K, pH 7) = 27±10 kJ mol^{-1}. Both methods show that the enolase reaction is an endothermic reaction, which was also validated by a calorimetric measurement, see Figure S1 in the SI. Please note that the heat production rate shown in Figure S1 is negative because we performed the reaction using PEP as a substrate, which is the product of the reaction regarding glycolysis. Thus, the negative value in Figure S1 yields a positive enthalpy of reaction.

Conclusion

Combination of equilibrium measurements and prediction of activity coefficients with ePC-SAFT were used to determine the thermodynamic equilibrium constant K_a' of the enolase reaction. K_a' was used to calculate the standard Gibbs energy of reaction $\Delta^R g'^0$, which is constant at any equilibrium composition at constant *T* and pH. K_a'(298.15 K, pH 7) and $\Delta^R g'^0$(298.15 K, pH 7) were determined in this work to be

3.2±0.2 and -2.8±0.2 kJ mol^{-1}, respectively. We found that the reaction equilibrium did not depend strongly on concentration in the considered concentration range up to 12 mmol kg^{-1} PEP. In contrast, the equilibrium of the enolase reaction depends strongly on pH, especially at pH values between 5 and 9. The $\Delta^R g'^0$ value at 298.15 K and pH 7 differs from literature $\Delta^R g'^{0,obs}$ values. This is not a surprising result as the data beyond postulated $\Delta^R g'^{0,obs}$ values from literature were measured often without providing the complete measuring conditions (concentrations, buffer type, pH, pMg). Thus, it might be argued that the postulated $\Delta^R g'^{0,obs}$ values from literature are reliable standard data. The reason behind the medium effect on reaction equilibrium is found by the activity coefficients of the reactant and products. This information is included in $\Delta^R g'^0$ value from the present work, and thus this value is recommended in all future works that are based on thermodynamic feasibility analysis of the glycolytic pathway.

Additionally, the standard enthalpy of reaction $\Delta^R h'^0$(298.15 K, pH 7) was determined from equilibrium measurements at 298.15 – 310.15 K to be 27±10 kJ mol^{-1} using the van ‘t Hoff equation. The reason behind the endothermic behavior was addressed by quantum-chemical calculations, which proved that an exothermic-endothermic shift occurs for dehydration reactions depending on the chain length of the reactant. Applying a new concept that replaces the biological species by model molecules allows accessing the enthalpy of reaction at the level of pure-component standard state in the liquid phase to be $\Delta^R h^0$(298.15 K) = 27±5 kJ mol^{-1}.

Appendix

Table 3: Osmotic coefficient ϕ of aqueous NaPEP solutions at pH 2.5, 273.15 K and 1 bar. pH was adjusted with NaOH which was considered in the determination of the osmotic coefficient (see eq. (16)).

m_{NaPEP}	ϕ
mol kg^{-1}	-
0.1000	0.8625
0.0800	0.8771
0.0700	0.8663
0.0583	0.8827
0.0499	0.8818
0.0400	0.9038
0.0299	0.9182

Table 4: Osmotic coefficient ϕ of aqueous NaPEP solutions at pH 5.1, 273.15 K and 1 bar. pH was adjusted with NaOH which was considered in the determination of the osmotic coefficient (see eq. (16)).

m_{NaPEP}	ϕ
mol kg^{-1}	-
0.1016	0.7803
0.0811	0.7924
0.0706	0.7946
0.0605	0.7924
0.0511	0.8000
0.0406	0.8194

0.0303	0.8429

Table 5: Osmotic coefficient ϕ of aqueous NaPEP solutions at pH 8.2, 273.15 K and 1 bar. pH was adjusted with NaOH which was considered in the determination of the osmotic coefficient (see eq. (16)).

m_{NaPEP}	ϕ
mol kg^{-1}	-
0.1018	0.7365
0.0812	0.7537
0.0714	0.7584
0.0609	0.7655
0.0508	0.7742
0.0398	0.7846
0.0303	0.7968

Table 6: Density ρ of aqueous NaPEP solutions at 298.15 K and 1 bar.

m_{NaPEP}	ρ
mol kg^{-1}	kg m^{-3}
0.1366	1011.5
0.0680	1004.4
0.0405	1001.4
0.0262	999.4

Accession ID for the enzyme enolase

Enolase was used from baker's yeast (UniProtKB - P00924).

Acknowledgement

This work was supported by the German Science Foundation (DFG) grant No. SA700/20-1 (Leibniz award to G. Sadowski) and grants HE7165/5-1, MA 3746/6-1 and VE 265/12-1 for the project "Glycolysis: thermodynamics and pathway predictions".

References

1. Maskow, T., and von Stockar, U. (2005) How reliable are thermodynamic feasibility statements of biochemical pathways?, *Biotechnol. Bioeng. 92,* 223–230.

2. Burton, K., and Krebs, H. A. (1953) The free-energy changes associated with the individual steps of the tricarboxylic acid cycle, glycolysis and alcoholic fermentation and with the hydrolysis of the pyrophosphate groups of adenosinetriphosphate, *Biochem. J. 54,* 94–107.

3. Mavrovouniotis, M. L. (1993) Identification of Localized and Distributed Bottlenecks in Metabolic Pathways, *Proc. Int. Conf. Intell. Syst. Mol. Biol. 1,* 275–283.

4. Vojinovic, V., and von Stockar, U. (2009) Influence of uncertainties in pH, pMg, activity coefficients, metabolite concentrations, and other factors on the analysis of the thermodynamic feasibility of metabolic pathways, *Biotechnol. Bioeng. 103,* 780–795.

5. Hoffmann, P., Held, C., Maskow, T., and Sadowski, G. (2014) A thermodynamic investigation of the glucose-6-phosphate isomerization, *Biophys. Chem. 195,* 22–31.

6. Gao, M., Held, C., Patra, S., Arns, L., Sadowski, G., and Winter, R. (2017) Crowders and Cosolvents-Major Contributors to the Cellular Milieu and Efficient Means to Counteract Environmental Stresses, *Chemphyschem 18,* 2951–2972.

7. Meurer, F., Bobrownik, M., Sadowski, G., and Held, C. (2016) Standard Gibbs Energy of Metabolic Reactions. I. Hexokinase Reaction, *Biochemistry 55,* 5665–5674.

8. Meurer, F., Do, H. T., Sadowski, G., and Held, C. (2017) Standard Gibbs energy of metabolic reactions. II. Glucose-6-phosphatase reaction and ATP hydrolysis, *Biophys. Chem. 223,* 30–38.

9. Wangler, A., Schmidt, C., Sadowski, G., and Held, C. (2018) Standard Gibbs Energy of Metabolic Reactions. III The 3-Phosphoglycerate Kinase Reaction, *ACS Omega 3,* 1783–1790.

10. Stryer, L. (1988) Biochemistry, W.H. Freeman and Co, New York.

11. Goldberg, R. N., and Tewari, Y. B. (1995) Thermodynamics of Enzyme-Catalyzed Reactions. Part 4. Lyases, *J. Phys. Chem. Ref. Data 24,* 1669–1698.

12. Alberty, R. A. (2003) Thermodynamics of biochemical reactions, Wiley-Interscience, Hoboken, N.J.

13. Meyerhof, O., and Oesper, P. (1949) The enzymatic equilibria of phospho(enol)pyruvate, *J. Biol. Chem. 179,* 1371–1385.

14. Warburg, O., and Christian, W. (1941) Isolierung und Kristallisation des Gärungsferments Enolase, *Naturwissenschaften 29,* 589–590.

15. Wold, F., and Ballou, C. E. (1956) Studies on the enzyme enolase. I. Equilibrium studies, *J. Biol. Chem. 227,* 301–312.

16. Garrett, R. H., and Grisham, C. M. (2013) Biochemistry. 5th ed., Brooks/Cole Cengage Learning, S.l.

17. Held, C., Reschke, T., Mohammad, S., Luza, A., and Sadowski, G. (2014) ePC-SAFT revised, *Chem. Eng. Res. Des. 92,* 2884–2897.

18. Gross, J., and Sadowski, G. (2001) Perturbed-Chain SAFT: An Equation of State Based on a Perturbation Theory for Chain Molecules, *Ind. Eng. Chem. Res. 40,* 1244–1260.

19. Held, C., and Sadowski, G. (2016) Thermodynamics of Bioreactions, *Annu. Rev. Chem. Biomol. Eng. 7,* 395–414.

20. Voges, M., Schmidt, F., Wolff, D., Sadowski, G., and Held, C. (2016) Thermodynamics of the alanine aminotransferase reaction, *Fluid Phase Equilibr. 422,* 87–98.

21. Wangler, A., Loll, R., Greinert, T., Sadowski, G., and Held, C. (2019) Predicting the high concentration co-solvent influence on the reaction equilibria of the ADH-catalyzed reduction of acetophenone, *J. Chem. Thermodyn. 128,* 275–282.

22. Voges, M., Abu, R., Gundersen, M. T., Held, C., Woodley, J. M., and Sadowski, G. (2017) Reaction Equilibrium of the ω-Transamination of (S)-Phenylethylamine: Experiments and ePC-SAFT Modeling, *Org. Process Res. Dev. 21,* 976–986.

23. Reed, G. H., Poyner, R. R., Larsen, T. M., Wedekind, J. E., and Rayment, I. (1996) Structural and mechanistic studies of enolase, *Curr. Opin. Struc. Biol. 6,* 736–743.

24. O'Leary, B., Park, J., and Plaxton, W. C. (2011) The remarkable diversity of plant PEPC (phosphoenolpyruvate carboxylase): recent insights into the physiological functions and post-translational controls of non-photosynthetic PEPCs, *Biochem. J. 436,* 15–34.

25. Cameretti, L. F., Sadowski, G., and Mollerup, J. M. (2005) Modeling of Aqueous Electrolyte Solutions with Perturbed-Chain Statistical Associated Fluid Theory, *Ind. Eng. Chem. Res. 44,* 3355–3362.

26. Held, C., Neuhaus, T., and Sadowski, G. (2010) Compatible solutes: Thermodynamic properties and biological impact of ectoines and prolines, *Biophys. Chem. 152,* 28–39.

27. Robinson, R. A., and Bower, V. E. (1965) Osmotic and Activity Coefficients of Tris(hydroxymethyl) aminomethane and Its Hydrochloride in Aqueous Solution at 25° C, *J. Chem. Eng. Data 10,* 246–247.

28. Fuchs, D., Fischer, J., Tumakaka, F., and Sadowski, G. (2006) Solubility of Amino Acids. Influence of the pH value and the Addition of Alcoholic Cosolvents on Aqueous Solubility, *Ind. Eng. Chem. Res. 45,* 6578–6584.

29. Frisch, M. J., Trucks, G. W., Schlegel, H. B., Scuseria, G. E., Robb, M. A., Cheeseman, J. R., Scalmani, G., Barone, V., Petersson, G. A., Nakatsuji, H., Li, X., Caricato, M., Marenich, A., Bloino, J., Janesko, B. G., Gomperts, R., Mennucci, B., Hratchian, H. P., Ortiz, J. V., Izmaylov, A. F., Sonnenberg, J. L., D. Williams-Young, Ding, F., Lipparini, F., Egidi, F., Goings, J., Peng, B., Petrone, A., Henderson, T., Ranasinghe, D., Zakrzewski, V. G., Gao, J., Rega, N., Zheng, G., Liang, W., Hada, M., Ehara, M., Toyota, K., Fukuda, R., Hasegawa, J., Ishida, M., Nakajima, T., Honda, Y.,

Kitao, O., Nakai, H., Vreven, T., Throssell, K., Montgomery, J. A., Jr., Peralta, J. E., Ogliaro, F., Bearpark, M., Heyd, J. J., Brothers, E., Kudin, K. N., Staroverov, V. N., Keith, T., Kobayashi, R., Normand, J., Raghavachari, K., Rendell, A., Burant, J. C., Iyengar, S. S., Tomasi, J., Cossi, M., Millam, J. M., Klene, M., Adamo, C., Cammi, R., Ochterski, J. W., Martin, R. L., Morokuma, K., Farkas, O., Foresman, J. B., and Fox, D. J. (2009) Gaussian 09, Revision A.02, Gaussian Inc, Wallingford CT.

30. Allinger, N. L., Yuh, Y. H., and Lii, J. H. (1989) Molecular mechanics. The MM3 force field for hydrocarbons. 1, *J. Am. Chem. Soc. 111,* 8551–8566.

31. Petersson, G. A., Bennett, A., Tensfeldt, T. G., Al-Laham, M. A., Shirley, W. A., and Mantzaris, J. (1988) A complete basis set model chemistry. I. The total energies of closed-shell atoms and hydrides of the first-row elements, *J. Chem. Phys. 89,* 2193–2218.

32. Curtiss, L. A., Redfern, P. C., and Raghavachari, K. (2007) Gaussian-4 theory, *J. Chem. Phys. 126,* 84108–84112.

33. Verevkin, S. P., Emel'yanenko, V. N., Notario, R., Roux, M. V., Chickos, J. S., and Liebman, J. F. (2012) Rediscovering the Wheel. Thermochemical Analysis of Energetics of the Aromatic Diazines, *J. Phys. Chem. Lett. 3,* 3454–3459.

34. Emel'yanenko, V. N., Zaitseva, K. V., Agapito, F., Martinho Simões, J. A., and Verevkin, S. P. (2015) Benchmark thermodynamic properties of methylanisoles: Experimental and theoretical study, *J. Chem. Thermodyn. 85,* 155–162.

35. Verevkin, S. P., Emel'yanenko, V. N., Diky, V., Muzny, C. D., Chirico, R. D., and Frenkel, M. (2013) New Group-Contribution Approach to Thermochemical Properties of

Organic Compounds: Hydrocarbons and Oxygen-Containing Compounds, *J. Phys. Chem. Ref. Data 42,* 33102.

36. Cox, J. D., Wagman, D. D., and Medvedev, V. A. (1984) CODATA Key Values for Thermodynamics, Hemisphere Publishing Corporation, New York.